Available online at www.sciencedirect.com
SCIENCE DIRECT®
Earth and Planetary Science Letters 244 (2006) 155–169
EPSL
www.elsevier.com/locate/epsl

Remelting of recently depleted mantle within the Hawaiian plume inferred from the ^{226}Ra–^{230}Th–^{238}U disequilibria of Pu‘u ‘Ō‘ō eruption lavas

Aaron J. Pietruszka [a,*], Erik H. Hauri [a], Richard W. Carlson [a], Michael O. Garcia [b]

[a] *Department of Terrestrial Magnetism, Carnegie Institution of Washington, 5241 Broad Branch Rd., N.W., Washington DC 20015, USA*
[b] *Department of Geology and Geophysics, University of Hawai‘i, 1680 East West Rd., Honolulu, HI 96822, USA*

Received 8 September 2005; received in revised form 15 January 2006; accepted 16 January 2006
Available online 21 February 2006
Editor: K. Farley

Abstract

Lavas from the Pu‘u ‘Ō‘ō eruption of Kīlauea Volcano are thought to partially bypass the shallow magma reservoir beneath the volcano’s summit, and thus, provide a relatively direct “window” to the mantle. Here we use high-precision U-series isotope measurements of Pu‘u ‘Ō‘ō lavas (1985–2001) to investigate the timing and mechanism of melt transport within the Hawaiian mantle plume. The lavas display small, but significant, temporal decreases in their ^{230}Th–^{238}U (~2.5% to 1.4% excess ^{230}Th) and ^{226}Ra–^{230}Th (~14% to 12% excess ^{226}Ra) disequilibria. These trends correlate systematically with larger decreases in abundance ratios of trace elements that are highly versus moderately incompatible during partial melting of the mantle. These ratios vary from a maximum of ~23% for Ba/Yb to a minimum of ~4% for Nd/Sm. Modeling of these geochemical signatures suggests that Pu‘u ‘Ō‘ō lavas are increasingly derived from a mantle source that was recently depleted by prior melt extraction within the Hawaiian plume. The timing of this depletion must be longer than the ~20-year duration of the eruption but less than several half-lives of ^{226}Ra (<8 kyr ago). A single magmatic process – the transfer of melt from pores in steady-state equilibrium with the residual mantle into chemically isolated channels – ultimately seems to control the rapid fluctuation in lava chemistry at Pu‘u ‘Ō‘ō. Specifically, this mode of melt extraction (if it occurs frequently) would create numerous patches of recently depleted mantle within Kīlauea’s source region that may subsequently remelt. When melt is extracted into channels to supply a given eruption, such as Pu‘u ‘Ō‘ō, it must be drained from an ever increasing volume in order to sustain the flow of melt to the surface. As the eruption continues, the volcano might tap melt from more distal areas and tend to encounter a greater number of patches of melt from recently depleted mantle. The source region of Pu‘u ‘Ō‘ō lavas within the Hawaiian plume is also thought to contain long-lived, small-scale compositional heterogeneities based on temporal variations of ratios of highly incompatible trace elements (Ba/Th or Th/U) and $^{87}Sr/^{86}Sr$. This melt-transport mechanism would allow Kīlauea to sample chemically and isotopically heterogeneous pockets of melt from “fresh” mantle that was never melted beneath Hawai‘i (in addition to melt from recently depleted mantle), and thus, efficiently transmit the geochemical signatures of these compositional heterogeneities from the volcano’s source region to the surface.

Keywords: Hawai‘i; Kīlauea Volcano; lava geochemistry; U-series isotopes; mantle melting; melt transport

* Corresponding author. Present address: Department of Geological Sciences, San Diego State University, 5500 Campanile Dr., San Diego, CA 92182-1020, USA. Tel.: +1 619 594 2648; fax: +1 619 594 4372.
E-mail address: apietrus@geology.sdsu.edu (A.J. Pietruszka).

0012-821X/$ - see front matter © 2006 Elsevier B.V. All rights reserved.
doi:10.1016/j.epsl.2006.01.039

1. Introduction

Partial melting of the mantle to produce ocean-island basalts and mid-ocean ridge basalts (MORB) is generally assumed to be a steady-state process in which the continuous flux of solid upwelling into the melting region is balanced, after melt generation and extraction, by the permanent removal of the residue from the system [1–3]. However, a theoretical model for oceanic spreading centers [4] suggests that the dynamics of melt transport in three dimensions may lead to the remelting of recently depleted mantle. The effects of such 3-D melt transport on the geochemical signatures of basalts are predicted to depend mostly on the type of mantle flow. Passive, plate-driven upwelling beneath the East Pacific Rise, causing melt to focus towards the spreading center and residue to diverge and remelt, is thought to control the distinctive trace-element compositions of on-versus off-axis MORB at 12° N [5]. Here we present an investigation of the geochemical effects of melt transport for the actively upwelling Hawaiian mantle plume using high-precision measurements of ^{226}Ra–^{230}Th–^{238}U disequilibria [6] in lavas from the Pu‘u ‘Ō‘ō eruption of Kīlauea Volcano.

Pu‘u ‘Ō‘ō lavas are ideally suited for a study of the geochemical effects of melt transport. Detailed petrologic studies [7–11] show that most Pu‘u ‘Ō‘ō lavas, except those from the early period of magma mixing (1983 to early 1985 [7,8]) and the short-duration (<1 day) Nāpau Crater eruption in January 1997 [10,11], are aphyric to weakly olivine phyric (<5% phenocrysts) and mafic (>7 wt.% MgO). These mafic lavas display compositional variations that are dominated by the fractionation and minor accumulation of olivine [8–10]. However, subtle changes in lava chemistry due to mantle processes are superimposed on the effects of olivine control. For example, previous studies [9,10] show that Pu‘u ‘Ō‘ō lavas display temporal decreases in their MgO-normalized abundances of CaO and highly incompatible elements. Modeling of these data suggests that Kīlauea has progressively tapped a mantle source that was depleted of incompatible elements and clinopyroxene by “recent” prior melting within the Hawaiian plume [9,10]. A possible explanation for these observations, based on the melt-transport model [4], is that active upwelling caused the buoyancy-driven recycling of depleted residue from the margin of the plume towards Kīlauea’s melting region, where it was subsequently remelted during the Pu‘u ‘Ō‘ō eruption. However, the choice of a physical mechanism to account for the compositional variations of Pu‘u ‘Ō‘ō lavas depends critically on the timing of the prior source depletion, which is poorly constrained by previous data. The ^{226}Ra–^{230}Th–^{238}U disequilibria of Pu‘u ‘Ō‘ō lavas, expressed as (^{230}Th)/(^{238}U) or (^{226}Ra)/(^{230}Th) ratios (parentheses indicate the activity, or decay rate, of each isotope), offer the potential to address this issue because the half-lives of these isotopes (~76 kyr for ^{230}Th and 1600 yr for ^{226}Ra) are thought to be similar to the time scale of magmatic processes.

Prior to melting, the source region of basaltic lavas will generally be in a state of radioactive equilibrium in which the (^{230}Th)/(^{238}U) and (^{226}Ra)/(^{230}Th) ratios are equal to unity because the daughter isotopes decay at the same rate as their (grand)parents. Any process that fractionates these elements, such as partial melting of the mantle, induces a state of disequilibrium in which the activities of ^{226}Ra, ^{230}Th and ^{238}U become unequal. Ratios of (^{230}Th)/(^{238}U) and (^{226}Ra)/(^{230}Th) greater than unity, such as those observed in Kīlauea lavas [12–15], denote excesses of the daughter isotopes, ^{230}Th and ^{226}Ra, relative to their (grand)parents, ^{238}U and ^{230}Th, respectively. These signatures are typically attributed to the “ingrowth” of the shorter-lived daughter isotopes during melt generation and extraction from a source originally in radioactive equilibrium within the Hawaiian plume [12–15].

Previous studies of Pu‘u ‘Ō‘ō lavas revealed small and constant ^{226}Ra–^{230}Th–^{238}U disequilibria [14,15] within the relatively large uncertainties of these TIMS (thermal ionization mass spectrometry) measurements. In contrast, the data presented in this study were collected using new analytical techniques developed for MC-ICP-MS (multiple-collector inductively coupled plasma mass spectrometry) with a precision that is a factor of ~2–3 better than TIMS [6]. This offers the potential to decipher subtle variations of (^{230}Th)/(^{238}U) and (^{226}Ra)/(^{230}Th) ratios. In addition to the ^{226}Ra–^{230}Th–^{238}U disequilibria, we use new measurements of the ^{87}Sr/^{86}Sr ratios and selected trace-element concentrations of these lavas to constrain the timing and mechanism of the prior source depletion at Pu‘u ‘Ō‘ō.

2. A brief overview of the Pu‘u ‘Ō‘ō eruption

The following history of the Pu‘u ‘Ō‘ō eruption is based on [7–11,16]. The eruption began on January 3, 1983 from a vent within Nāpau Crater on Kīlauea’s east rift zone and quickly formed a ~7.5-km long fissure. By June 1983, the eruption became localized to a single vent (Pu‘u ‘Ō‘ō) and was characterized by short periods of high lava fountaining (typically <24 h long) separated by repose periods (24 days long on average). In July 1986, a new vent (Kūpaianaha) located 3 km further

down the rift zone formed. Kūpaianaha was the site of nearly continuous lava effusion until February 1992. The locus of effusion returned to Pu'u 'Ō'ō in the middle of February 1992. Subsequently, lava effusion at Pu'u 'Ō'ō has been nearly continuous except for a brief (<1 day long) eruption from a fissure within Nāpau Crater in January 1997, which was accompanied by a 24-day hiatus in activity. The eruption is continuing as of January 2006.

3. Analytical methods

High-precision measurements of the Ba, Th, U, Sr, Nd, Sm, Yb and ^{226}Ra concentrations and (^{230}Th)/(^{232}Th), (^{234}U)/(^{238}U) and ^{87}Sr/^{86}Sr ratios of selected Pu'u 'Ō'ō lavas (Tables 1 and 2) and two Hawaiian rock standards (Table 3), Kil1919 and BHVO-2, were performed by mass spectrometry at the Carnegie Institution of Washington. All elemental abundances were determined by isotope dilution. Sr concentrations and isotopic ratios were measured by TIMS on a VG 354. All other measurements were performed using MC-ICP-MS on a VG P54-30. All uncertainties in this paper are $\pm 2\sigma$, unless otherwise noted. The general MC-ICP-MS operating conditions and the details of the analytical techniques for ^{226}Ra, Th and U measurements (both elemental abundances and isotope ratios) are described by [6]. Ba, Sr, Nd, Sm and Yb were separated from the wash of the sample solution used to determine the Th and U concentrations with a column of AG50W-X8 cation exchange resin by sequential elution of Sr followed by Yb in 2.5 M HCl, Ba in 2 M HNO_3, and Nd and Sm along with most other rare-earth elements in 4 M HCl. Nd and Sm were subsequently purified using a column of Eichrom LN Resin in 0.2 M HCl (for Nd) followed by 0.75 M HCl (for Sm). Sr isotope ratios were corrected for instrumental mass fractionation relative to ^{86}Sr/^{88}Sr = 0.1194 using the exponential law [17]. Sr isotope ratios were measured over two periods of time that gave different ^{87}Sr/^{86}Sr values for the NBS987 Sr standard: 0.710291 ± 26 (n = 34) and 0.710260 ± 33 (n = 15). Data for samples run during the first period were corrected relative to the second period (a decrease of 0.000031). All data are reported relative to ^{87}Sr/^{86}Sr = 0.710260 for the NBS987 Sr standard. Within-run uncertainties on individual ^{87}Sr/^{86}Sr measurements were less than the external reproducibility of SRM987. The measured ^{87}Sr/^{86}Sr ratios of Kil1919 and BHVO-2 agree closely with previous analyses summarized in Table 3 [15,18,19]. Total procedural blanks, Ba (<2.6 ng), Sr (<280 pg), Nd (<30 pg), Sm (<50 pg) and Yb (<10 pg), were negligible.

4. Results

Pu'u 'Ō'ō lavas display small, but significant, temporal decreases in their ^{230}Th–^{238}U and ^{226}Ra–^{230}Th disequilibria from ~2.5% to 1.4% excess ^{230}Th and ~14% to 12% excess ^{226}Ra (Fig. 1). These changes in the (^{230}Th)/(^{238}U) and (^{226}Ra)/(^{230}Th) ratios correlate systematically with larger decreases in abundance ratios of trace

Table 1
U-series isotope and other geochemical data for lavas from the Pu'u 'Ō'ō eruption of Kīlauea Volcano, Hawai'i

Sample	$^{226}Ra_0^a$ (pg g^{-1})	Ba (μg g^{-1})	Th (μg g^{-1})	U (μg g^{-1})	Sr (μg g^{-1})	Nd (μg g^{-1})	Sm (μg g^{-1})	Yb (μg g^{-1})	(^{230}Th/^{232}Th)	(^{234}U/^{238}U)	^{87}Sr/^{86}Sr
KE30-362 #1[b]	0.1189±10[c]	114.0	0.9044	0.3023	334.2	20.08	5.229	1.980	1.0395±13[d]	1.0004±4	0.703580±11
KE30-362 #2		114.2	0.9116	0.3040	334.2	20.21	5.260	1.990			
16-Mar-87	0.1172±10	112.6	0.8949	0.2985	336.0	20.22	5.300	2.033	1.0362	1.0012±11	0.703579±8
26-Mar-89	0.1155±8	110.0	0.8848	0.2962	336.2	20.54	5.436	2.107	1.0372±33	1.0013±10	0.703597±16
12-May-91		107.1	0.8692	0.2918	335.0	20.38	5.437	2.123			0.703603±10
29-Dec-92 #1	0.1107±7	103.4	0.8459	0.2852	326.4	19.86	5.305	2.084	1.0431±7	1.0009±9	0.703593±16
29-Dec-92 #2		100.7	0.8217	0.2767	317.0	19.29	5.158	2.030			
27-Apr-95	0.1132±8	105.9	0.8675	0.2923	334.9	20.43	5.463	2.146	1.0421±6	1.0010±4	0.703613±14
13-Feb-99 #1	0.1082±9	101.4	0.8300	0.2794	323.3	19.59	5.273	2.101	1.0387±23	1.0016±5	0.703612±5
13-Feb-99 #2	0.1046±9	99.03	0.8092	0.2721	317.2	19.11	5.148	2.053	1.0361	1.0014±7	0.703620±12
21-Jun-00 #1	0.1024±7	97.20	0.7901	0.2665	315.6	18.93	5.149	2.074	1.0389±17	1.0016±7	0.703647±8
21-Jun-00 #2		98.18	0.7977	0.2692	318.2	19.10	5.195	2.095			
8-Jan-01	0.1035±9	98.43	0.7997	0.2697	319.0	19.12	5.199	2.089	1.0375	1.0006±35	0.703636±13

[a]The ^{226}Ra concentrations are corrected for post-eruptive decay. [b]This sample was collected ~15 m from the vent on 8-Feb-85 [8], but probably erupted on 5-Feb-85. [c]Uncertainties on the ^{226}Ra concentrations are ±2 standard deviations of the mean ($\pm 2\sigma_m$) for the within-run measured ratios. [d]Uncertainties on the Th, U and Sr isotope ratios are based on the $\pm 2\sigma_m$ (n > 2) or total range (n = 2) of replicate analyses. The individual analyses are reported in Table 2.

Table 2
Individual Th, U and Sr isotope ratio analyses for lavas from the Pu‘u ‘Ō‘ō eruption of Kīlauea Volcano, Hawai‘i

Sample	(^{230}Th/^{232}Th)	(^{234}U/^{238}U)	^{87}Sr/^{86}Sr
KE30-362 #1	1.0382	1.0001	0.703576
	1.0401	1.0008	0.703566
	1.0402	1.0003	0.703585
			0.703592
16-Mar-87	1.0362	1.0007	0.703570
		1.0018	0.703584
			0.703587
			0.703574
26-Mar-89	1.0389	1.0013	0.703583
	1.0355	1.0002	0.703617
		1.0005	0.703601
		1.0031	0.703586
		1.0013	
12-May-91			0.703608
			0.703613
			0.703589
			0.703602
29-Dec-92 #1	1.0434	1.0010	0.703582
	1.0424	1.0004	0.703577
	1.0435	1.0002	0.703586
		1.0004	0.703585
		1.0026	0.703628
			0.703602
27-Apr-95	1.0417	1.0015	0.703623
	1.0424	1.0005	0.703633
		1.0007	0.703596
		1.0011	0.703610
		1.0013	0.703601
13-Feb-99 #1	1.0373	1.0015	0.703607
	1.0409	1.0013	0.703621
	1.0378	1.0021	0.703613
			0.703607
			0.703614
13-Feb-99 #2	1.0361	1.0018	0.703626
		1.0011	0.703603
			0.703620
			0.703630
21-Jun-00 #1	1.0398	1.0009	0.703654
	1.0372	1.0011	0.703642
	1.0396	1.0021	0.703631
		1.0024	0.703649
			0.703662
			0.703646
			0.703641
8-Jan-01	1.0375	1.0023	0.703652
		0.9988	0.703649
			0.703651
			0.703605
			0.703620
			0.703654
			0.703623
			0.703629

elements that are highly versus moderately incompatible during partial melting of the mantle. These ratios vary from a maximum of ~23% for Ba/Yb (not shown) to a minimum of ~4% for Nd/Sm (Fig. 1). The variations of these trace-element ratios are analogous to the temporal decreases in the MgO-normalized abundances of highly incompatible elements that were previously noted for Pu‘u ‘Ō‘ō lavas [9,10]. The Ba/Th and Th/U ratios decreased slightly, but significantly, for the older lavas with a distinct flattening of the Th/U ratio and reversal of the Ba/Th ratio for the younger lavas. Thus, the (^{230}Th)/(^{238}U) and (^{226}Ra)/(^{230}Th) ratios of the older lavas correlate systematically with their closest geochemical analogs, Th/U (for ^{230}Th–^{238}U disequilibria) and Ba/Th (for ^{226}Ra–^{230}Th disequilibria), but the younger lavas depart from these trends. The ^{87}Sr/^{86}Sr ratios increased over time from ~0.70358 to 0.70364.

5. Evaluation of traditional models

In this section, we evaluate a range of traditional magmatic processes that might account for the compositional variations of Pu‘u ‘Ō‘ō lavas (Fig. 1).

5.1. Crustal assimilation

A possible explanation for the temporal decreases of the (^{230}Th)/(^{238}U) and (^{226}Ra)/(^{230}Th) ratios of Pu‘u ‘Ō‘ō lavas is the progressive assimilation of crustal materials that had partially or completely reached radioactive equilibrium. Since radioactive decay will cause any ^{230}Th–^{238}U or ^{226}Ra–^{230}Th disequilibrium in a zero-age lava to return towards equilibrium on a time scale of the half-life of the shorter-lived isotope in each pair, modeling the effects of bulk crustal assimilation is straightforward. Ancient crust, such as old lavas within Kīlauea’s volcanic edifice or underlying Mauna Loa lavas, will have (^{230}Th)/(^{238}U) and (^{226}Ra)/(^{230}Th) ratios close to unity. Progressive assimilation of such crust would cause a trend that departs strongly from the observed correlation (R^2=0.92) between the (^{226}Ra)/(^{230}Th) and (^{230}Th)/(^{238}U) ratios of Pu‘u ‘Ō‘ō lavas (Fig. 2a). Thus, any crust being assimilated by Kīlauea must be young relative to the half-life of ^{226}Ra. The amount of excess ^{226}Ra and ^{230}Th in this young crust must be equal to or less than the smallest values observed during the Pu‘u ‘Ō‘ō eruption in order to account for the temporal trends towards smaller ^{226}Ra–^{230}Th–^{238}U disequilibria. For our calculation (Fig. 2a), we assume that zero-age crust has a (^{226}Ra)/(^{230}Th) ratio of 1.14 (equal to KE30-362) and a (^{230}Th)/(^{238}U) ratio of 1.014 (the lowest value observed at Kīlauea [15]). Assuming a different amount of excess ^{226}Ra for the zero-age crust only changes the required age of the crust being assimilated. Next, the (^{226}Ra)/

Table 3
Sr isotope ratios and trace-element abundances for Hawaiian rock standards

Sample	Ba ($\mu g\ g^{-1}$)	Th ($\mu g\ g^{-1}$)	U ($\mu g\ g^{-1}$)	Sr ($\mu g\ g^{-1}$)	Nd ($\mu g\ g^{-1}$)	Sm ($\mu g\ g^{-1}$)	Yb ($\mu g\ g^{-1}$)	$^{87}Sr/^{86}Sr$
Kil1919 #4[a]	134.6	1.220	0.4255	394.1	24.67	6.099	2.026	0.703456
Kil1919 #5		1.221	0.4258					0.703474
Kil1919 #6	134.6	1.221	0.4264	393.9	24.70	6.105	2.028	0.703469
Kil1919 #7	135.7	1.228	0.4279	395.3	24.84	6.140	2.039	0.703490
Average								0.703472
$\pm 2\sigma$								0.000028
Literature[b] ($n=3$)								0.703473[c]
$\pm 2\sigma$								0.000001
BHVO-2	131.4	1.195	0.4177	386.2	24.24	6.009	2.003	0.703485
Literature[d] ($n=3$)								0.703486[c]
$\pm 2\sigma$								0.000017

[a] The numbers after each replicate analysis of Kil1919 correspond to the analyses of these standards for ^{226}Ra, Th and U abundances and $(^{230}Th)/(^{232}Th)$ and $(^{234}U)/(^{238}U)$ ratios reported in [6].
[b] The literature value for Kil1919 is the average of data from [15,18].
[c] Literature data are corrected relative to the $^{87}Sr/^{86}Sr$ ratio of NBS987 for this study (0.710260).
[d] The literature value for BHVO-2 is the average of the leached analyses from [19].

(^{230}Th) and (^{230}Th)/(^{238}U) ratios of the zero-age crust are adjusted for a range of ages according to the decay equation. Mixing lines are calculated between this variably aged crust and sample KE30-362, which would represent the least contaminated Pu‘u ‘Ō‘ō magma. Assimilation of ~300 year old crust can account for the data, but this is unlikely because ~100% contamination would be required to match the youngest Pu‘u ‘Ō‘ō lava. Even if the zero-age crust is assumed to be in ^{230}Th–^{238}U equilibrium (an end member for the least amount of crustal assimilation), >50% contamination would still be required (not shown). Instead, we conclude that the variations of the ^{226}Ra–^{230}Th–^{238}U disequilibria, and other geochemical parameters in Pu‘u ‘Ō‘ō lavas (Fig. 1), are not due to crustal assimilation.

5.2. Magma mixing

Magma mixing is known to be an important control on the compositional variations of Pu‘u ‘Ō‘ō lavas prior to February 1985. Lavas from the start of the eruption in January 1983 were evolved (<7 wt.% MgO) hybrids with petrographic and geochemical evidence of mixing between two differentiated, rift-zone stored magmas [7]. Subsequently, Pu‘u ‘Ō‘ō lavas became increasingly more mafic as this differentiated magma was flushed from a ~0.05 km^3 reservoir [20] within the rift-zone by a mafic (~9–10 wt.% MgO) magma derived from the volcano’s summit reservoir [8]. Modeling shows that the amount of the differentiated, rift-zone stored hybrid magma reached 0% by January 1985 [8]. All of the samples studied here are mafic lavas with >7 wt.% MgO that erupted after this early period of magma mixing at Pu‘u ‘Ō‘ō. Lavas from the 1997 Nāpau Crater eruption, which were likely stored within Kīlauea’s rift zone for an extended period of time [10,11], were excluded. For the remainder of this paper, we use the term “Pu‘u ‘Ō‘ō lavas” to refer to samples erupted after January 1985 (excluding those from the 1997 Nāpau Crater eruption).

Since February 1985, Pu‘u ‘Ō‘ō lavas display systematic temporal decreases in their MgO-normalized abundances of CaO and highly incompatible elements that are thought to reflect changes in the composition of the parental magma delivered to the volcano [9,10]. The rate of these variations in lava chemistry is a factor of ~3 faster than observed in historical lavas from the volcano’s summit region [8]. This observation led to the idea that Pu‘u ‘Ō‘ō lavas may partially bypass the shallow, ~2–3 km^3 magma reservoir [21] beneath the summit of Kīlauea, and thus, provide a relatively direct “window” to the mantle [9]. The geochemical signatures of these lavas (Fig. 1) cannot be explained by simple two-component mixing of mafic magmas because some of the parameters display monotonic temporal trends (top row) but others do not (bottom row). Instead, any magma mixing (if it occurred) would require more than two mafic components that were mixed on a time scale that was much shorter than the ~20-year duration of the eruption. Regardless of the role of magma mixing after January 1985 at Pu‘u ‘Ō‘ō, the differences in lava chemistry shown on Fig. 1 must ultimately result from mantle processes (since crustal assimilation is an unlikely explanation for the data).

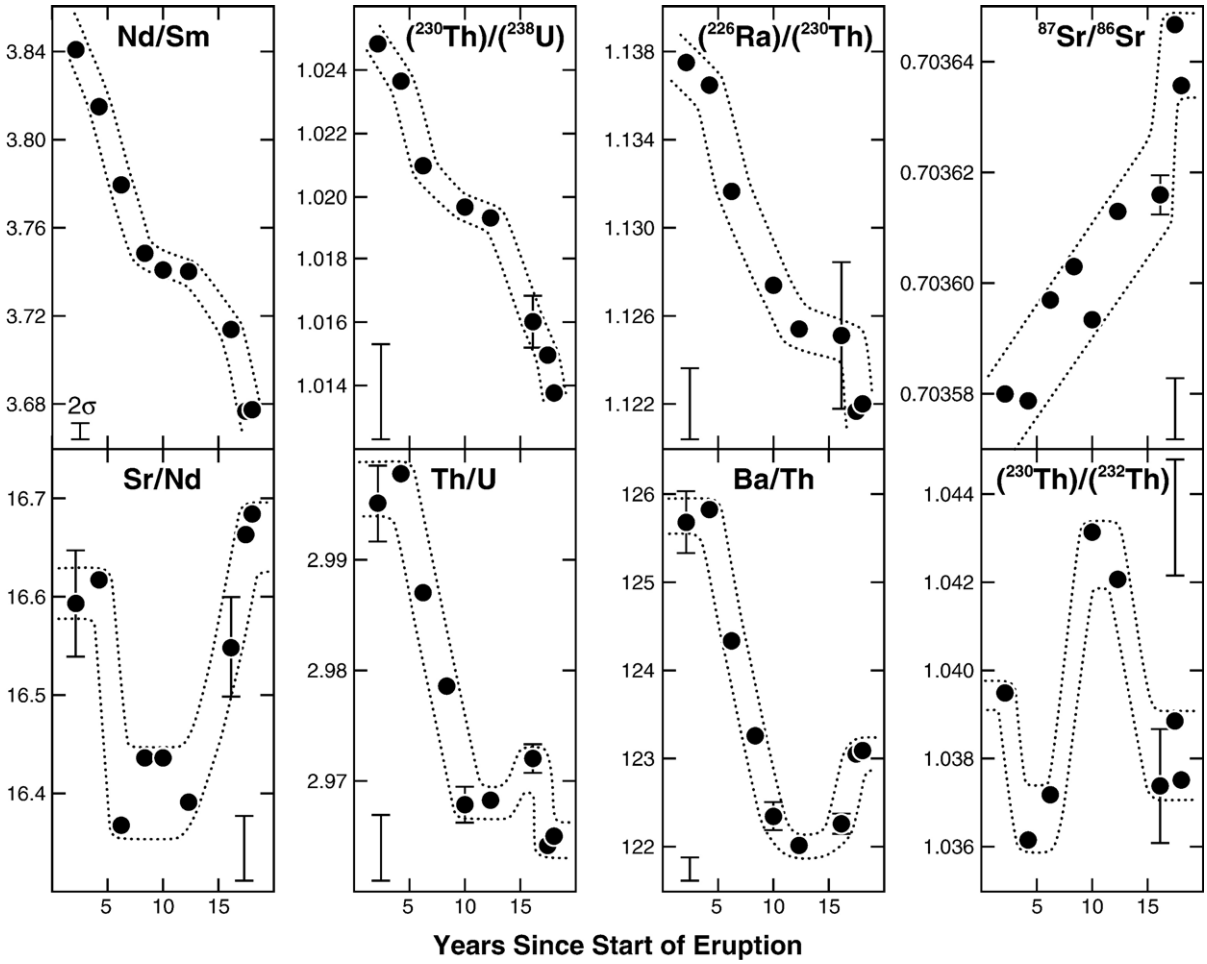

Fig. 1. Temporal geochemical variations of Pu'u 'Ō'ō lavas. Error bars ($\pm 2\sigma$) based on replicate analyses of Kil1919 (Table 3), except for the $^{87}Sr/^{86}Sr$ ratios, are shown in a corner of each plot unless they are smaller than the size of the symbols. The error bar for the $^{87}Sr/^{86}Sr$ ratios is the maximum $\pm 2\sigma_m$ value based on the replicate analyses in Table 2. Error bars on individual symbols show the reproducibility of independent duplicate analyses from Table 1.

5.3. An increase in the degree of partial melting

A simple explanation for many of the geochemical signatures of Pu'u 'Ō'ō lavas is an increase in the degree of partial melting. For example, a ~20% relative increase in the melt fraction during the sustained Mauna Ulu rift-zone eruption of Kīlauea was proposed based on systematic temporal decreases in the MgO-normalized abundances of highly incompatible elements in the lavas [22]. A similar model for Pu'u 'Ō'ō lavas was rejected [9,10] because (1) there has been no increase in the magma supply rate during the eruption, which would be expected from an increase in the melt fraction [9] and (2) an increase in the degree of partial melting cannot account for the temporal decreases of highly incompatible trace-element ratios, such as Ba/Ce [10] or Th/U and Ba/Th for the oldest Pu'u 'Ō'ō lavas (Fig. 1), given the relatively high melt fractions expected for Kīlauea lavas [18]. Instead, the variations of highly incompatible trace-element and $^{87}Sr/^{86}Sr$ ratios (Fig. 1) require temporal changes in the composition of the mantle source tapped by the volcano.

An increase in the melt fraction might explain the temporal decreases of the ^{226}Ra–^{230}Th–^{238}U disequilibria, despite the evidence for source heterogeneity from the Th/U and Ba/Th ratios, because the $(^{230}Th)/(^{238}U)$ and $(^{226}Ra)/(^{230}Th)$ ratios of basalts are expected to be independent of any long-lived trace-element heterogeneity in the mantle source [these pairs will be in radioactive equilibrium after ~8 kyr for ^{226}Ra–^{230}Th and ~380 kyr for ^{230}Th–^{238}U]. This idea was tested using the end-member time-independent models of batch and accumulated fractional melting [23]. The results of these calculations (Fig. 2b) show that the

^{226}Ra–^{230}Th–^{238}U disequilibria of Pu‘u ‘Ō‘ō lavas do not plot along melting trends, which must pass through (^{230}Th)/(^{238}U) and (^{226}Ra)/(^{230}Th) ratios of unity at high degrees of partial melting (for a source in radioactive equilibrium prior to melting), regardless of the Ra, Th and U partition coefficients assumed for the model. Instead, the (^{230}Th)/(^{238}U) and (^{226}Ra)/(^{230}Th) ratios of the lavas show a trend (R^2 = 0.92) that projects towards ~10% excess ^{226}Ra when ^{230}Th is in radioactive equilibrium with ^{238}U.

This problem can potentially be solved using time-dependent, or “ingrowth”, models that take into account the time scale of the melting process through additional parameters, such as the melting rate and the porosity of the melting region [1–3]. The temporal decreases of the (^{230}Th)/(^{238}U) and (^{226}Ra)/(^{230}Th) ratios might reflect increases in the melting rate and melt-zone porosity, respectively (Fig. 2b). Since neither parameter exerts a significant effect on stable incompatible trace-element ratios [3], an increase in the melt fraction would also be required to explain the temporal decreases in ratios of highly versus moderately incompatible trace elements. In addition, a realistic model would have to account for the short-term changes in source composition observed at Pu‘u ‘Ō‘ō based on the temporal fluctuations of the Ba/Th, Th/U and ^{87}Sr/^{86}Sr ratios (Fig. 1). Thus, a successful ingrowth model would require a delicate balance between the melting rate, the melt-zone porosity and the melt fraction (superimposed on the short-term changes in source composition) in order to account for the variations in lava chemistry at Pu‘u ‘Ō‘ō.

This requirement is inconsistent with two important features of the Pu‘u ‘Ō‘ō data (Fig. 1). First, the distinct, and somewhat irregular, temporal fluctuations of the Th/U and (^{230}Th)/(^{232}Th) ratios combine to produce a systematic decrease of the (^{230}Th)/(^{238}U) ratio

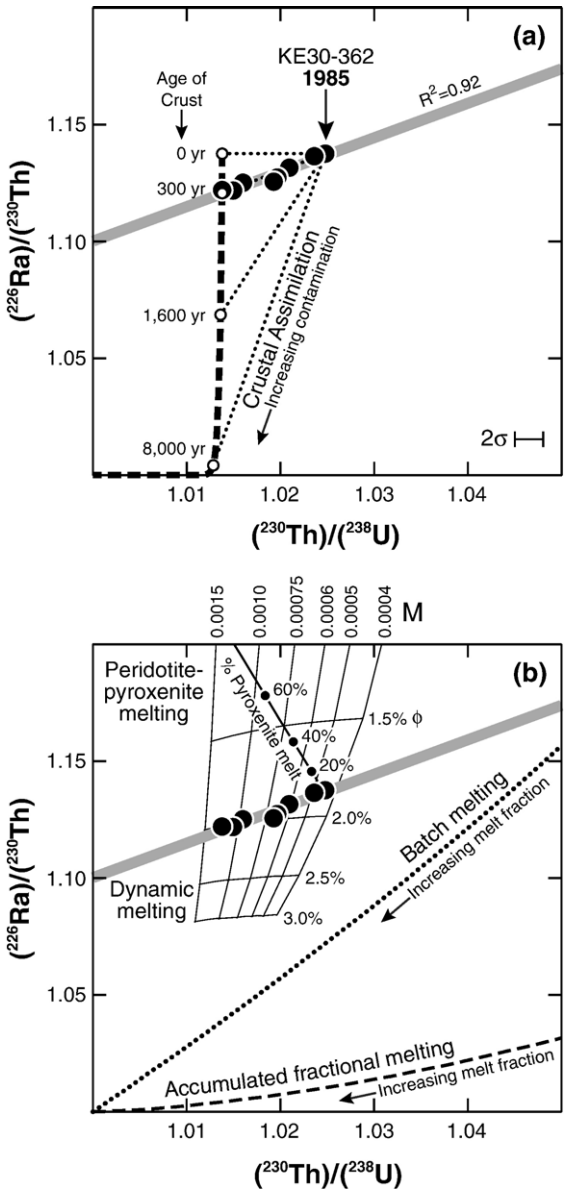

Fig. 2. Ratio–ratio plot of (^{230}Th)/(^{238}U) vs. (^{226}Ra)/(^{230}Th) for Pu‘u ‘Ō‘ō lavas (large black circles). (a). Crustal assimilation. The heavy dashed line shows the temporal changes in the ^{226}Ra–^{230}Th–^{238}U disequilibria of hypothetical crust (small open circles). Progressive contamination of the oldest Pu‘u ‘Ō‘ō lava with this crust would create mixtures that lie along the dotted lines. (b). Melting models. Melting trends for time-independent models [23] are shown as a dotted line (batch melting) or dashed line (accumulated fractional melting) for variable degrees of partial melting. Unless otherwise noted, model calculations shown on this figure assume the source mineralogy and bulk partition coefficients described in Appendix A. The result of the time-dependent dynamic melting model [1,2] is shown as a contoured grid for different values of the melting rate (M: kg m^{-3} yr^{-1}) and melt-zone porosity (ϕ: vol.%) at a constant melt fraction of 10%. A peridotite-pyroxenite melt mixing trend is shown by the solid line with small black circles at 20% increments of pyroxenite melt. For pyroxenite melting, a source mineralogy of 75% clinopyroxene and 25% garnet is assumed. Partition coefficients for Ra (=Ba), Th and U in pyroxenite are taken from [26] because these values are thought to be more appropriate for pyroxenite melting [25]. A constant 7.5 cm/yr rate of mantle upwelling, a melt-column height of 55 km and the dynamic melting model [1,2] are assumed for the calculation (similar results are obtained using the equilibrium percolation model [3]). Assuming a melt fraction of 10%, this upwelling rate translates to a melting rate of 0.00045 kg m^{-3} yr^{-1}. At this melting rate and a melt-zone porosity of ~1.8%, the (^{230}Th)/(^{238}U) and (^{226}Ra)/(^{230}Th) ratios of the oldest Pu‘u ‘Ō‘ō lava (KE30-362) can be explained by melting a peridotite source. The melt productivity of pyroxenite is assumed to be a factor of ~4 greater than peridotite. Thus, a melt fraction of 40% was used for the pyroxenite source, which translates to a melting rate of 0.0018 kg m^{-3} yr^{-1} (at the same 7.5 cm/yr mantle upwelling rate). Error bars are derived as described in Fig. 1. The error bar for (^{226}Ra)/(^{230}Th) is smaller than the size of the symbols.

during the eruption. Second, the (^{226}Ra)/(^{230}Th) ratio decreases systematically over time despite the reversal in the temporal trend of the Ba/Th ratio (a geochemical analog). These observations suggest that the variation of the (^{226}Ra)/(^{230}Th), (^{230}Th/^{238}U), and other strongly correlated ratios, such as Nd/Sm, are controlled by a single magmatic process that largely overwhelms any compositional differences due to source heterogeneity [which may affect the Th/U, (^{230}Th)/(^{232}Th) and Ba/Th ratios]. Ingrowth melting is an unlikely explanation for the geochemical signatures of Pu‘u ‘Ō‘ō lavas because a single, simple physical mechanism that would link each of the parameters required by a successful model is unknown.

5.4. Peridotite-pyroxenite melting

Progressive mixing of a low-degree, incompatible-element enriched melt from a peridotite source with an increasing proportion of a high-degree, incompatible-element depleted melt from a pyroxenite source has been proposed to explain the compositional variations of Pu‘u ‘Ō‘ō lavas [24]. This hypothesis can be tested using an ingrowth model and the (^{230}Th)/(^{238}U) and (^{226}Ra)/(^{230}Th) ratios of Pu‘u ‘Ō‘ō lavas because the partition coefficients for Th and U are thought to differ significantly between peridotite and pyroxenite [25,26], such that a pyroxenite melt is expected to have a low (^{230}Th)/(^{238}U) ratio and a high (^{226}Ra)/(^{230}Th) ratio compared to a peridotite melt. The smaller amount of excess ^{230}Th in pyroxenite melt results from the similarity of D_{Th} and D_U for clinopyroxene in pyroxenite, which reduces the Th–U fractionation. The greater amount of excess ^{226}Ra results from the higher D_{Th} for clinopyroxene in pyroxenite, which increases the Ra–Th fractionation. Assuming that an increasing amount of a pyroxenite melt is added to an early peridotite melt (KE30-362), the mixing trend would depart from the Pu‘u ‘Ō‘ō data towards smaller ^{230}Th–^{238}U and larger ^{226}Ra–^{230}Th disequilibria (Fig. 2b). This inverse trend does not depend strongly on the model parameters (aside from the choice of the partition coefficients) or the type of ingrowth model [1–3]. Thus, mixing of peridotite versus pyroxenite melts cannot account for the geochemical signatures of Pu‘u ‘Ō‘ō lavas, unless the assumed partition coefficients are incorrect.

6. Recent prior melting of Kīlauea’s source region

Previous studies [9,10] have suggested that Kīlauea has progressively tapped a mantle source during the Pu‘u ‘Ō‘ō eruption that was depleted of incompatible elements by “recent” prior melting within the Hawaiian plume. The dominant geochemical signatures of this prior source depletion and subsequent remelting in Pu‘u ‘Ō‘ō lavas are the temporal decreases in the MgO-normalized abundances of highly incompatible elements [9,10] and ratios of highly versus moderately incompatible trace elements (Fig. 1). Given the relative incompatibility of Ra, Th and U during partial melting of the mantle beneath Kīlauea ($D_{Ra} < D_{Th} < D_U$) [15], the trends toward smaller amounts of excess ^{230}Th and ^{226}Ra over time are consistent with the temporal decreases in both the trace-element ratios and abundances. Qualitatively, this may result from the fact that a depleted residue, and thus, a partial melt of this residue, will have relatively low abundances of highly incompatible elements and low ratios of highly versus moderately incompatible elements. Furthermore, this melt will have relatively low ratios of highly incompatible elements, such as Ba/Th and Th/U, and if the prior depletion and subsequent remelting occurred recently, large deficits of ^{230}Th and ^{226}Ra. Thus, the temporal trends towards smaller amounts of excess ^{226}Ra and ^{230}Th in Pu‘u ‘Ō‘ō lavas are consistent with the interpretation of previous studies [9,10]. The systematic correlations between the ^{226}Ra–^{230}Th–^{238}U disequilibria and trace-element ratios such as Nd/Sm (Fig. 1) show that the prior depletion and subsequent remelting must have occurred within several half-lives of ^{226}Ra (~8 kyr). This time scale may be used to constrain the mechanism of melt transport beneath Kīlauea.

A theoretical model for oceanic spreading centers [4] suggests that active upwelling of the mantle might lead to the remelting of recently depleted mantle due to the buoyancy-driven recycling of residue back into the melting region. Although this is strictly a 2-D model intended for MORB, it provides a potential mechanism to account for the geochemical signatures of Pu‘u ‘Ō‘ō lavas. Given the interpretation of this melt-transport model shown in Fig. 3, active upwelling within the Hawaiian plume might cause a parcel of depleted residue near the margin of the plume to travel on a roughly circular path from the point where it leaves the top of the melting region to the point where it re-enters the melting region from below. If this residue is assumed to be recycled from the margin of the plume towards Kīlauea’s melting region, the minimum distance it travels before re-entering the melting region would be ~50% of the circumference of a circle with a radius approximately equal to the distance between Kīlauea and the location of prior melting. Lō‘ihi Seamount [27] and Mauna Loa Volcano [28,29] may tap mantle that is

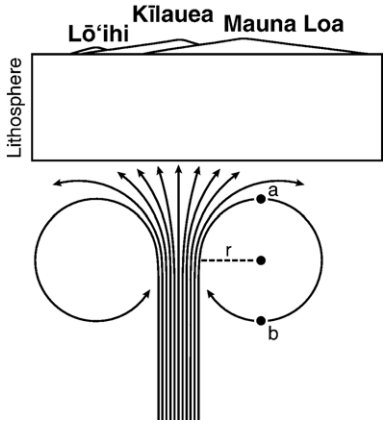

Fig. 3. Schematic model for the flow of mantle within the Hawaiian plume (lines with arrows) based on a 2-D melt-transport model for oceanic spreading centers [4]. The "*r*" refers to the radius of the circular path a parcel of depleted residue near the margin of the plume might travel from the point where it leaves the top of the melting region ("a") to the point where it re-enters the melting region from below ("b").

melting near the margins of the Hawaiian plume, and thus, represent potential sites for the development of the residue. Given distances of ~50 km (Kīlauea-Lō'ihi) and ~30 km (Kīlauea-Mauna Loa) and estimates for the rates of mantle upwelling beneath Lō'ihi (~20–40 cm/yr) and Mauna Loa (~30–70 cm/yr) [14], the minimum time scale of recycling would be >100 kyr. Thus, the geochemical signature of depletion in Pu'u 'Ō'ō lavas (<8 kyr old based on their ^{226}Ra–^{230}Th disequilibria) is probably far too young to result from the buoyancy-driven recycling of residue.

Similarly, depletion of the volcano's source region, and subsequent remelting, during the ~20-year duration of the eruption itself is unlikely. Even with a relatively high estimate for the melting rate at Kīlauea (~0.03 kg m^{-3} yr^{-1} [15]), it would take >1000 years to produce only ~1% of new melt. This is inconsistent with the relatively high degree of partial melting expected for Kīlauea lavas [18]. Instead, the depletion most likely occurred within Kīlauea's melting region in the more distant past.

Models for melt transport within the mantle typically range from the slow percolation of melt in chemical equilibrium with the residue [3] to the rapid flow of melt in chemically isolated channels [1,2]. Numerical models [30–34], petrologic observations of abyssal peridotites and the mantle portions of ophiolites [35], and geochemical data from MORB [36–38] indicate that both mechanisms of melt transport operate simultaneously in the mantle beneath oceanic spreading centers. Both types of melt transport are probably important beneath Hawai'i. However, the transfer of melt from pores in steady-state equilibrium with the residual mantle into chemically isolated channels may be the dominant mode of melt extraction for Kīlauea because (1) it is an efficient means of depleting the volcano's source region and producing heterogeneous patches of recently depleted mantle, and (2) it quickly provides a relatively large volume of melt, which would make it possible to supply high-output eruptions like Pu'u 'Ō'ō (~0.1 km^3/yr).

The importance of the melt-supply issue can be illustrated with simple mass-balance calculations. For example, a 55-km tall [15] and 1-km wide cylinder of upwelling mantle with a melt-zone porosity of 2% would contain ~0.9 km^3 of melt available for rapid extraction into channels. It would take ~2000 years to extract the same amount of melt by equilibrium percolation from a melting region of the same size assuming a relatively high melting rate of 0.03 kg m^{-3} yr^{-1} as a best-case scenario. Alternately, a 14-km wide cylinder of upwelling mantle (55-km tall) and a melting rate of 0.03 kg m^{-3} yr^{-1} would be required to supply melt to Kīlauea at the observed eruption rate for Pu'u 'Ō'ō (~0.1 km^3/yr) by equilibrium percolation. The total volume of this melting region would be ~8500 km^3. Such a large melting region for Kīlauea (and other Hawaiian volcanoes) is difficult to reconcile with the evidence for long-lived, small-scale heterogeneities within the Hawaiian plume based on studies of olivine-hosted melt inclusions from Mauna Loa lavas [39], the short-term fluctuations of Pb, Sr and Nd isotope ratios in historical lavas from Kīlauea [18] and Mauna Loa [40], and fine-scale Pb isotopic variations at individual Hawaiian volcanoes [41,42].

We envision the following melt-transport mechanism for Kīlauea (Fig. 4). Generally, the mantle beneath Hawai'i rises to the surface with melt percolating upwards in steady-state equilibrium with the residue. However, the transfer of this melt from pores into chemically isolated channels may be the most important mode of melt extraction, particularly for sustained, high output eruptions like Pu'u 'Ō'ō. If this process occurs frequently at Kīlauea (and other Hawaiian volcanoes), it will create numerous patches of recently depleted mantle beneath Hawai'i. Assuming the rate of mantle upwelling near the axis of the Hawaiian plume is ~10 m/yr (based on modeling of ^{226}Ra–^{230}Th–^{238}U disequilibria in Kīlauea summit lavas [15] and a fluid dynamical model [43]), it would take only ~5500 years to completely replace a 55-km tall melting region with "fresh" mantle (i.e., mantle that was never melted

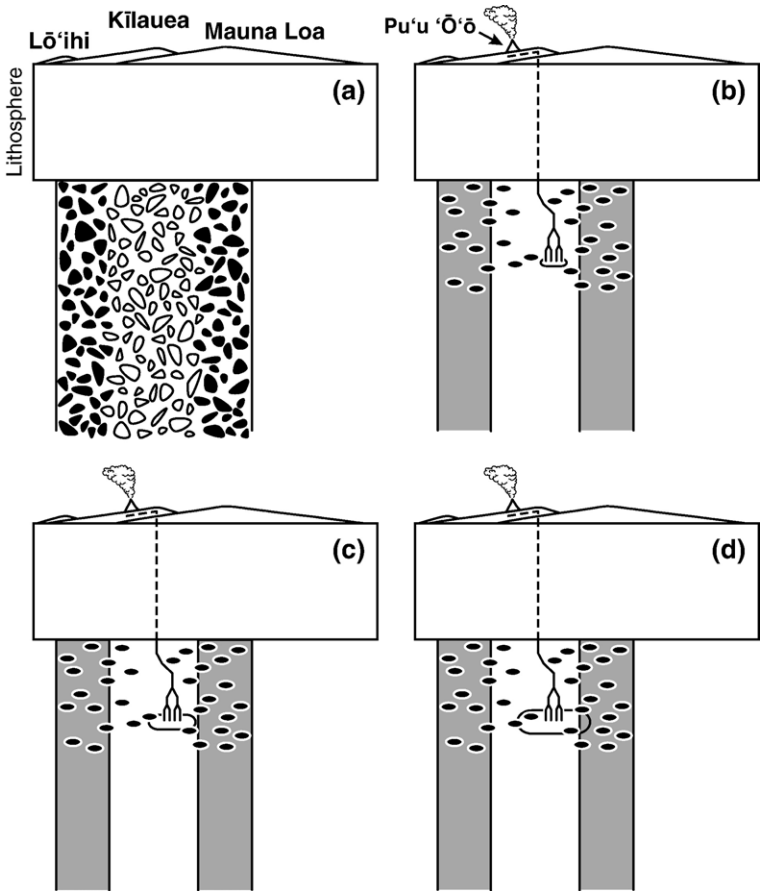

Fig. 4. Schematic melting model for the Pu'u 'Ō'ō eruption. (a). The uppermost portion of the Hawaiian mantle plume is stippled with black and white blobs that represent small-scale, long-lived compositional heterogeneities [18,39–42]. These heterogeneities are shown with a large-scale radial zonation, but other geometries are possible (e.g., bilateral asymmetry [42]). As this mantle rises to the surface, melt percolates upward in steady-state equilibrium with the residue. (b). The transfer of melt from pores into chemically isolated channels to supply eruptions at Lō'ihi, Kīlauea and Mauna Loa in the past may have created patches of recently depleted mantle beneath Hawai'i (small black ovals). The Pu'u 'Ō'ō eruption, illustrated by the small vent, dashed melt pathway and inverted fractal "tree", represents a current example of this process. Initially, the Pu'u 'Ō'ō eruption may have tapped fresh mantle that was never melted beneath Hawai'i (small elongate region at the base of the fractal tree). The small-scale, long-lived compositional heterogeneities from (a) are simplified to white and gray bands for clarity. (c). When melt is extracted into channels to supply a given eruption, such as Pu'u 'Ō'ō, it must be drained from an ever increasing volume in order to sustain the flow of melt to the surface. As the eruption continues, the volcano might tap melt from more distal areas and tend to encounter a greater number of patches of melt from recently depleted mantle (medium elongate region that overlaps with the black ovals). (d). As this process continues, the volcano might sample chemically and isotopically heterogeneous pockets of melt from fresh mantle (in addition to melt from recently depleted mantle), and thus, efficiently transmit the geochemical signatures of long-lived, small-scale compositional heterogeneities from the volcano's source region to the surface (large elongate region that overlaps with the black ovals and the shaded area).

beneath Hawai'i) from below. Since the mantle upwelling rate beneath Hawai'i is thought to decrease exponentially from the axis of the plume towards its margin [14,15,43], any recently depleted mantle will be replaced more slowly farther from the plume axis. When melt is extracted into channels to supply a given eruption, such as Pu'u 'Ō'ō, it must be drained from an ever increasing volume in order to sustain the flow of melt to the surface. As the eruption continues, the volcano might tap melt from more distal areas and tend to encounter a greater number of patches of melt from recently depleted mantle. This single, simple mechanism of melt transport would allow residue that was depleted by recent prior melting within the Hawaiian plume to remelt before it is permanently removed from the system. Furthermore, it would allow Kīlauea to sample chemically and isotopically heterogeneous pockets of melt from fresh mantle (in addition to melt from recently depleted mantle), and thus, efficiently transmit the geochemical signatures of long-lived,

small-scale compositional heterogeneities from the volcano's source region to the surface.

A model of recent prior melting has also been proposed for MORB [44] based on (1) the wide variation in the (^{230}Th)/(^{232}Th) ratios of normal MORB compared to relatively constant tracers of long-lived source heterogeneity, such as ^{87}Sr/^{86}Sr ratios, and (2) in inverse correlation between the (^{230}Th)/(^{232}Th) ratios of East Pacific Rise MORB and trace-element indices of source depletion, such as Rb/Sr ratios. In contrast to the depletion of Kīlauea's source region within the last ~8 kyr (based on the ^{226}Ra–^{230}Th disequilibria of Pu'u 'Ō'ō lavas), the recent prior melting for MORB must be much older in order to affect the (^{230}Th)/(^{232}Th) ratios of the lavas (given the ~76 kyr half-life of ^{230}Th). These geochemical signatures of MORB are thought to reflect multiple episodes of melt extraction at the spreading center with an approximate recurrence interval of ~100–300 kyr [44].

7. A quantitative melting model for Pu'u 'Ō'ō lavas

No ingrowth models are available to simulate the mechanism of melt transport that we propose for Kīlauea. Both of the simple end-member ingrowth models, dynamic [1,2] or equilibrium percolation [3] melting, assume that the continuous flux of solid upwelling into the melting region (a one-dimensional melt column) is balanced, after melt generation and extraction, by the permanent removal of the residue from the system. During dynamic melting, the column holds a constant porosity of melt that remains in chemical equilibrium with the residue, but all melt in excess of this porosity is instantaneously removed from the residue (at all depths in the column, simultaneously) and mixed together. In contrast, the melt and residue continuously interact as the melt moves up the column during equilibrium percolation melting. In both cases, this process results in a variably depleted residue (increasingly depleted from the bottom to the top), but chemical equilibrium between the percolating melt and residue is maintained continuously (until the residue is permanently removed from the system). Thus, neither model allows for the remelting of recently depleted mantle. Second, the

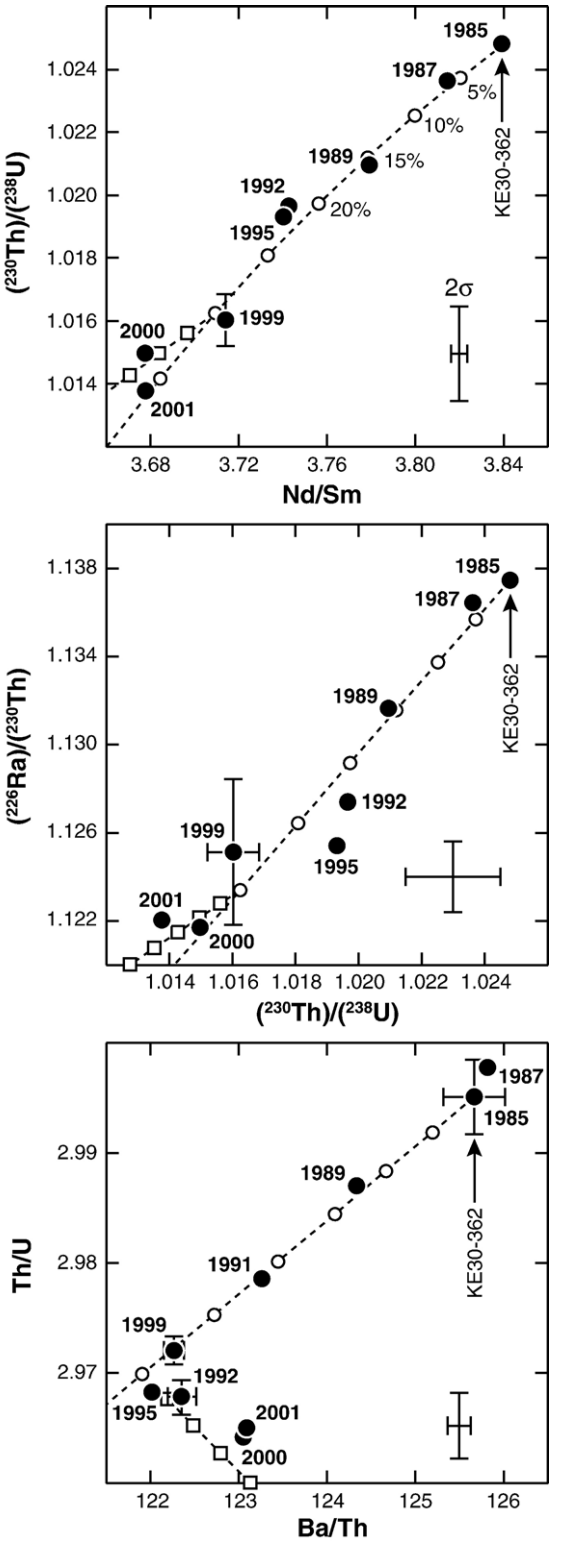

Fig. 5. Ratio–ratio plots of Nd/Sm vs. (^{230}Th)/(^{238}U), (^{230}Th)/(^{238}U) vs. (^{226}Ra)/(^{230}Th) and Ba/Th vs. Th/U for Pu'u 'Ō'ō lavas (black circles). Mixing trends with open circles show 5% additions of melt from recently depleted mantle to the oldest Pu'u 'Ō'ō lava (KE30-362). Mixing trends with open squares represent 5% additions of equal parts of melt from recently depleted mantle and melt from fresh mantle with the average composition of historical Mauna Loa lavas [12–14,40]. This Mauna Loa melt is assumed to have Nd/Sm ~3.55, Ba/Th ~150, Th/U ~2.96, and 2% and 15% excesses of ^{230}Th and ^{226}Ra, respectively. Error bars are derived as described in Fig. 1.

assumption of steady-state requires that the composition of the mantle entering the melting region remains constant over time (whether or not this mantle is in radioactive equilibrium prior to melting). Although this is a situation that can be applied to a fresh portion of the melting region (since the upwelling mantle will be always be in radioactive equilibrium), it is impossible to apply either model to a source that has experienced recent prior melting.

Accordingly, we modified existing models (Appendix A) to produce two hypothetical melts (a melt from fresh mantle and a melt formed by the remelting of recently depleted mantle). The oldest lava (KE30-362 from February 1985) is modeled to represent melt that was extracted from fresh mantle. An appropriate composition for the melt from recently depleted mantle was calculated in two steps. First, the composition of this residue was estimated by assuming that the interstitial melt (modeled to match KE30-362 using the equilibrium percolation melting model [3]) was in equilibrium with the residue before it was completely extracted. Second, the composition of the melt produced from this residue was calculated using a 2600-year duration of remelting. This calculation shows that the residue, and thus, partial melts of it, will have low (^{230}Th)/(^{238}U), (^{226}Ra)/(^{230}Th), Ba/Th, Th/U, and Nd/Sm ratios (the melt has Nd/Sm ~3.2, Ba/Th ~12, Th/U ~2.4, and 18% and 29% deficits of ^{230}Th and ^{226}Ra, respectively).

Mixing between a melt from fresh mantle and an increasing proportion of melt from recently depleted mantle matches the temporal decreases in the (^{230}Th)/(^{238}U), (^{226}Ra)/(^{230}Th), Ba/Th, Th/U, and Nd/Sm ratios of the older Pu‘u ‘Ō‘ō lavas (Fig. 5). In addition, remelting explains the temporal decrease in the Sr/Nd ratios of the older lavas because partial melts of the residue will have low Sr/Nd ratios ($D_{Sr}<D_{Nd}$ during partial melting at Kīlauea [18]). This process also accounts for the lower Nd/Sm ratios and smaller ^{226}Ra–^{230}Th–^{238}U disequilibria of the younger Pu‘u ‘Ō‘ō lavas. However, the temporal flattening of the Th/U ratio, the reversals of the Ba/Th and Sr/Nd ratios, and the increase of the ^{87}Sr/^{86}Sr ratio over time cannot be explained solely by the incorporation of melt from a source that has experienced recent prior depletion because (1) these trace-element ratios would be much lower in partial melts of the residue than observed in any Pu‘u ‘Ō‘ō lavas and (2) the ^{87}Sr/^{86}Sr ratios would not be affected by a recent process. Instead, an influx of melt from a fresh source within the Hawaiian plume that is compositionally and isotopically distinct from the source of the older Pu‘u ‘Ō‘ō lavas is required (in addition to more melt from recently depleted mantle). Although the Pu‘u ‘Ō‘ō geochemical signatures are within the historical range known for Kīlauea [15,18], the younger lavas trend towards the composition of historical Mauna Loa lavas, which possess relatively high Ba/Th, Sr/Nd and ^{87}Sr/^{86}Sr ratios, but similar Th/U ratios, compared to Kīlauea [12–14,40]. Mixing calculations show that the addition of melt with the average composition of historical Mauna Loa lavas (in addition to melt from recently depleted mantle) will account for the geochemical signatures of the younger Pu‘u ‘Ō‘ō lavas (Fig. 5).

8. Conclusions

Lavas from the Pu‘u ‘Ō‘ō eruption display small, but significant, temporal decreases in their ^{230}Th–^{238}U and ^{226}Ra–^{230}Th disequilibria that correlate systematically with larger decreases in ratios of highly versus moderately incompatible trace elements. Modeling of these geochemical signatures suggests that Pu‘u ‘Ō‘ō lavas are increasingly derived from a mantle source that was recently depleted by prior melt extraction within the Hawaiian plume. The timing of this depletion must be longer than the ~20-year duration of the eruption but less than several half-lives of ^{226}Ra (<8 kyr ago). A single magmatic process – the transfer of melt from pores in steady-state equilibrium with the residual mantle into chemically isolated channels – ultimately seems to control the rapid fluctuation in lava chemistry at Pu‘u ‘Ō‘ō. If this mode of melt extraction occurs frequently at Kīlauea (and other Hawaiian volcanoes), it will create numerous patches of recently depleted mantle beneath Hawai‘i that may subsequently remelt. When melt is extracted into channels to supply a given eruption, such as Pu‘u ‘Ō‘ō, it must be drained from an ever increasing volume in order to sustain the flow of melt to the surface. As the eruption continues, the volcano might tap melt from more distal areas and tend to encounter a greater number of patches of melt from recently depleted mantle. The source region of Pu‘u ‘Ō‘ō lavas within the Hawaiian plume is also thought to contain long-lived, small-scale compositional heterogeneities based on temporal variations of ratios of highly incompatible trace elements (Ba/Th or Th/U) and ^{87}Sr/^{86}Sr. This melt-transport mechanism would allow Kīlauea to sample chemically and isotopically heterogeneous pockets of melt from fresh mantle (in addition to melt from recently depleted mantle), and thus, efficiently transmit the geochemical signatures of these compositional heterogeneities from the volcano’s source region to the surface.

Acknowledgements

This research was completed under the auspices of a Carnegie Institution of Washington Postdoctoral Research Fellowship to A. Pietruszka and a grant from the National Science Foundation to M. Garcia and A. Pietruszka (EAR 03-36874). The helpful comments of F. Frey, V. Camp and an anonymous reviewer are gratefully acknowledged.

Appendix A. Details of the melting model for Pu‘u ‘Ō‘ō lavas

We assume that the oldest Pu‘u ‘Ō‘ō lava (KE30-362) represents melt that was extracted into chemically isolated channels from pores in steady-state equilibrium with fresh mantle. After extraction, this melt is assumed to mix and erupt instantaneously. The composition of this melt is calculated from the equilibrium percolation melting model [3]. Specifically, the melt contained within the pores of a steady-state column of upwelling mantle undergoing equilibrium percolation melting is integrated using the output of the UserCalc program [45], which is a numerical solution to the equations of [3]. The UserCalc program returns the porosity (%), the total degree of partial meting experienced by the solid, and the $(^{230}Th)/(^{238}U)$ and $(^{226}Ra)/(^{230}Th)$ ratios of melt within the pores at known, but uneven, depth intervals ($n=20$) throughout the melting region. The ^{226}Ra and ^{230}Th abundances of the melt within each depth interval are calculated from the output ^{226}Ra–^{230}Th–^{238}U disequilibria and the ^{238}U concentrations (the latter are determined as described below, assuming ^{238}U behaves like a stable trace element). The composition of the melt within the pores at each depth interval is weighted according to the thickness of the depth interval and its porosity to derive the integrated melt composition.

In this way, the $(^{230}Th)/(^{238}U)$ and $(^{226}Ra)/(^{230}Th)$ ratios of KE30-362 can be reproduced (Fig. 5) with an upwelling rate of 667 cm/yr (equivalent to a melting rate of 0.08 kg m^{-3} yr^{-1}), a maximum degree of partial melting of 20%, a melt-column height of 55 km, a maximum porosity of 3.3% and a source in radioactive equilibrium prior to melting. The average degree of partial melting (appropriate for the interstitial melt) is equal to 50% of the maximum degree of partial melting (i.e., 10%). A source mineralogy of 60% olivine, 15% clinopyroxene, 15% orthopyroxene and 10% garnet is assumed. Bulk partition coefficients were calculated using D values compiled in [18] except for Th and U. We assume $D_{Th}=D_U=0.005$ in clinopyroxene from [46] and $D_{Th}=0.0157$ and $D_U=0.024$ in garnet, which lie within the range of the data in [46]. The abundances of the stable trace elements in melt extracted from fresh mantle were calculated assuming the same parameters used to model the ^{226}Ra–^{230}Th–^{238}U disequilibria, source concentrations of Ba (8.9 μg/g), Th (0.077 μg/g), U (0.026 μg/g), Nd (3.0 μg/g) and Sm (0.95 μg/g), and the batch melting model [23]. The equilibrium percolation melting model is mathematically equivalent to batch melting for stable trace elements [3].

The composition of the recently depleted mantle was estimated from the output of the UserCalc program assuming the interstitial melt that was modeled to match KE30-362 (as described above) was in equilibrium with the residual solid before it was completely extracted. This results in a variably depleted residue, and a trend of decreasing depletion with increasing depth in the melting region. Since the concentration of ^{226}Ra, ^{230}Th and ^{238}U in the depleted residue of equilibrium percolation melting is governed by the same mathematical formula as the residue of batch melting [3], determination of the $(^{230}Th)/(^{238}U)$, $(^{226}Ra)/(^{230}Th)$ and stable trace-element ratios of the depleted residue is straightforward. The average composition of the depleted residue is determined by integrating over the entire melting region, using the output of the UserCalc program as described previously.

Simulating the remelting of the recently depleted mantle in a way that takes into account the duration of partial melting (as required to understand the effects on ^{226}Ra–^{230}Th–^{238}U disequilibria) is difficult. We approximate the composition of melt from this source using the average composition of the depleted residue (after the extraction of the melt that is modeled to match KE30-362) and the equations for batch melting [23]. Ingrowth of ^{226}Ra towards radioactive equilibrium with ^{230}Th as melting progresses is determined simply by the decay equation. Ingrowth of ^{230}Th is ignored. This is likely to be a close approximation to the actual melt composition because (1) equilibrium percolation melting is equivalent to batch melting for stable trace elements [3], (2) the duration of remelting is probably much shorter than the half-life of ^{230}Th, and (3) the amount of ^{226}Ra–^{230}Th–^{238}U disequilibrium produced during ingrowth melting at Kīlauea is thought to be relatively small [12–15]. The UserCalc program is used only to estimate the vertical profile of melt fraction and porosity that would redevelop as this depleted residue continues to rise towards the surface, using the same assumptions described previously except for a smaller maximum degree of partial melting (12.4%). All other parameters are the same as assumed for the production

of melt from fresh mantle. Again, the average abundances of the short-lived isotopes (^{226}Ra and ^{230}Th) and stable trace elements (including ^{238}U) are calculated by integrating the melt contained within the pores of this column of upwelling mantle. Finally, an extended duration of melting (2600 yr) inferred from the average degree (6.2%) and rate (0.08 kg m^{-3} yr^{-1}) of melting is used to account for the ingrowth of ^{226}Ra prior to the second episode of melt extraction.

References

[1] D. McKenzie, ^{230}Th–^{238}U disequilibrium and the melting processes beneath ridge axes, Earth Planet. Sci. Lett. 72 (1985) 149–157.

[2] R.W. Williams, J.B. Gill, Effects of partial melting on the uranium decay series, Geochim. Cosmochim. Acta 53 (1989) 1,607–1,619.

[3] M. Spiegelman, T. Elliott, Consequences of melt transport for uranium series disequilibrium in young lavas, Earth Planet. Sci. Lett. 118 (1993) 1–20.

[4] M. Spiegelman, Geochemical consequences of melt transport in 2-D: the sensitivity of trace elements to mantle dynamics, Earth Planet. Sci. Lett. 139 (1996) 115–132.

[5] M. Spiegelman, J.R. Reynolds, Combined dynamic and geochemical evidence for convergent melt flow beneath the East Pacific Rise, Nature 402 (1999) 282–285.

[6] A.J. Pietruszka, R.W. Carlson, E.H. Hauri, Precise and accurate measurement of ^{226}Ra–^{230}Th–^{238}U disequilibria in volcanic rocks using plasma ionization multicollector mass spectrometry, Chem. Geol. 188 (2002) 171–191.

[7] M.O. Garcia, R.A. Ho, J.M. Rhodes, E.W. Wolfe, Petrologic constraints on rift-zone processes: results from episode 1 of the Pu‘u ‘Ō‘ō eruption of Kīlauea Volcano, Hawai‘i, Bull. Volcanol. 52 (1989) 81–96.

[8] M.O. Garcia, J.M. Rhodes, E.W. Wolfe, G.E. Ulrich, R.A. Ho, Petrology of lavas from episodes 2–47 of the Pu‘u ‘Ō‘ō eruption of Kīlauea Volcano, Hawai‘i: evaluation of magmatic processes, Bull. Volcanol. 55 (1992) 1–16.

[9] M.O. Garcia, J.M. Rhodes, F.A. Trusdell, A.J. Pietruszka, Petrology of lavas from the Pu‘u ‘Ō‘ō eruption of Kīlauea Volcano: III. The Kūpaianaha episode (1986–1992), Bull. Volcanol. 58 (1996) 359–379.

[10] M.O. Garcia, A.J. Pietruszka, J.M. Rhodes, K. Swanson, Magmatic processes during the prolonged Pu‘u ‘Ō‘ō eruption of Kīlauea Volcano, Hawai‘i, J. Petrol. 41 (2000) 967–990.

[11] C.R. Thornber, C. Heliker, D.R. Sherrod, J.P. Kauahikaua, A. Miklius, P.G. Okubo, F.A. Trusdell, J.R. Budahn, W.I. Ridley, G.P. Meeker, Kīlauea east rift zone magmatism: a episode 54 perspective, J. Petrol. 44 (2003) 1,525–1,559.

[12] A.S. Cohen, R.K. O’Nions, Melting rates beneath Hawai‘i: evidence from uranium series isotopes in recent lavas, Earth Planet. Sci. Lett. 120 (1993) 169–175.

[13] C. Hémond, A.W. Hofmann, G. Heusser, M. Condomines, I. Raczek, J.M. Rhodes, U–Th–Ra systematics in Kīlauea and Mauna Loa basalts, Hawai‘i, Chem. Geol. 116 (1994) 163–180.

[14] K.W.W. Sims, D.J. DePaolo, M.T. Murrell, W.S. Baldridge, S. Goldstein, D. Clague, M. Jull, Porosity of the melting zone and variations in the solid mantle upwelling rate beneath Hawai‘i: inferences from the ^{238}U–^{230}Th–^{226}Ra and ^{235}U–^{231}Pa disequilibria, Geochim. Cosmochim. Acta. 63 (1999) 4,119–4,138.

[15] A.J. Pietruszka, K.H. Rubin, M.O. Garcia, ^{226}Ra–^{230}Th–^{238}U disequilibria of historical Kīlauea lavas (1790–1982) and the dynamics of mantle melting within the Hawaiian plume, Earth Planet. Sci. Lett. 186 (2001) 15–31.

[16] C. Heliker, T.N. Mattox, The first two decades of the Pu‘u ‘Ō‘ō-Kūpaianaha eruption: chronology and selected bibliography, in: C. Heliker, D.A. Swanson, T.J. Takahashi (Eds.), The Pu‘u ‘Ō‘ō-Kūpaianaha Eruption of Kīlauea Volcano, Hawai‘i: The First 20 Years, US Geol. Surv. Prof. Pap., vol. 1676, 2003, pp. 1–28.

[17] W.A. Russell, D.A. Papanastassiou, T.A. Tombrello, Ca isotope fractionation on the Earth and other solar system materials, Geochim. Cosmochim. Acta 42 (1978) 1,075–1,090.

[18] A.J. Pietruszka, M.O. Garcia, A rapid fluctuation in the mantle source and melting history of Kīlauea Volcano inferred from the geochemistry of its historical summit lavas (1790–1982), J. Petrol. 40 (1999) 1,321–1,342.

[19] D. Weis, B. Kieffer, C. Maerschalk, W. Pretorius, J. Barling, High-precision Pb–Sr–Nd–Hf isotopic characterization of USGS BHVO-1 and BHVO-2 reference materials, Geochem. Geophys. Geosyst. 6 (2005), doi:10.1029/2004GC000852.

[20] P.J. Shamberger, M.O. Garcia, Geochemical modeling of magma mixing and magma reservoir volumes during early episodes of Kīlauea Volcano’s Pu‘u ‘Ō‘ō eruption, Bull. Volcanol. (in press).

[21] A.J. Pietruszka, M.O. Garcia, The size and shape of Kīlauea Volcano’s summit magma storage reservoir: a geochemical probe, Earth Planet. Sci. Lett. 167 (1999) 311–320.

[22] A.W. Hofmann, M.D. Feigenson, I. Raczek, Case studies on the origin of basalt: III, petrogenesis of the Mauna Ulu eruption, Kīlauea, 1969–1971, Contrib. Mineral. Petrol. 88 (1984) 24–35.

[23] D.M. Shaw, Trace element fractionation during anatexis, Geochim. Cosmochim. Acta 34 (1970) 237–243.

[24] P.W. Reiners, Temporal-compositional trends in intraplate basalt eruptions: implications for mantle heterogeneity and melting processes, Geochem. Geophys. Geosyst. 3 (2002), doi:10.1029/2001GC000250.

[25] A. Stracke, V.J.M. Salters, K.W.W. Sims, Assessing the presence of garnet-pyroxenite in the mantle sources of basalts through combined hafnium–neodymium–thorium isotope systematics, Geochem. Geophys. Geosyst. 1 (1999), doi:10.1029/1999GC000013.

[26] E.H. Hauri, T.P. Wagner, T.L. Grove, Experimental and natural partitioning of Th, U, Pb and other trace elements between garnet, clinopyroxene and basaltic melts, Chem. Geol. 117 (1994) 149–166.

[27] J.G. Moore, D.A. Clague, W.R. Normark, Diverse basalt types from Lō‘ihi seamount, Hawai‘i, Geology 10 (1982) 88–92.

[28] M.D. Kurz, T.C. Kenna, D.P. Kammer, J.M. Rhodes, M.O. Garcia, Isotopic evolution of Mauna Loa Volcano: a view from the submarine southwest rift zone, in: J.M. Rhodes, J.P. Lockwood (Eds.), Mauna Loa Revealed: Structure, Composition, History, and Hazards, AGU, Geophys. Monogr., vol. 92, 1995, pp. 289–306.

[29] P.W. Lipman, Declining growth of Mauna Loa during the last 100,000 years: rates of lava accumulation vs. gravitational subsidence, in: J.M. Rhodes, J.P. Lockwood (Eds.), Mauna Loa Revealed: Structure, Composition, History, and Hazards, AGU, Geophys. Monogr., vol. 92, 1995, pp. 45–80.

[30] D. McKenzie, The generation and compaction of partially molten rock, J. Petrol. 25 (1984) 713–765.

[31] N.H. Sleep, Tapping of melt by veins and dikes, J. Geophys. Res. 93 (1988) 10,255–10,272.
[32] D.J. Stevenson, Spontaneous small-scale melt segregation in partial melts undergoing deformation, Geophys. Res. Lett. 16 (1989) 1,067–1,070.
[33] E. Aharonov, J.A. Whitehead, P.B. Kelemen, M. Spiegelman, Channeling instability of upwelling melt in the mantle, J. Geophys. Res. 100 (1995) 20,433–20,450.
[34] M. Spiegelman, P.B. Kelemen, E. Aharonov, Causes and consequences of flow organization during melt transport: the reaction infiltration instability in compactible media, J. Geophys. Res. 106 (2001) 2,061–2,077.
[35] P.B. Kelemen, N. Shimizu, V.J.M. Salters, Extraction of mid-ocean-ridge basalt from the upwelling mantle by focused flow of melt in dunite channels, Nature 375 (1995) 747–753.
[36] C. Lundstrom, Models of U-series disequilibria generation in MORB: the effect of two scales of melt porosity, Phys. Earth Planet. Inter. 121 (2000) 189–204.
[37] M. Jull, P.B. Kelemen, K. Sims, Consequences of diffuse and channeled porous melt migration on uranium series disequilibria, Geochim. Cosmochim. Acta 66 (2002) 4,133–4,148.
[38] K.W.W. Sims, S.J. Goldstein, J. Blichert-Toft, M.R. Perfit, P. Keleman, D.J. Fournari, P. Michael, M.T. Murrell, S.R. Hart, D.J. DePaolo, G. Layne, L. Ball, M. Jull, J. Bender, Chemical and isotopic constraints on the generation and transport of magma beneath the East Pacific Rise, Geochim. Cosmochim. Acta 66 (2002) 3,481–3,504.
[39] A.V. Sobolev, A.W. Hofmann, I.K. Nikogosian, Recycled oceanic crust observed in “ghost plagioclase” within the source of Mauna Loa lavas, Nature 404 (2000) 986–990.
[40] J.M. Rhodes, S.R. Hart, Episodic trace element and isotopic variations in historical Mauna Loa lavas: implications for magma and plume dynamics, in: J.M. Rhodes, J.P. Lockwood (Eds.), Mauna Loa Revealed: Structure, Composition, History, and Hazards, AGU, Geophys. Monogr., vol. 92, 1995, pp. 263–288.
[41] J. Eisele, W. Abouchami, S.J.G. Galer, A.W. Hofmann, The 320 kyr Pb isotope evolution of Mauna Kea lavas recorded in the HSDP-2 drill core, Geochem. Geophys. Geosyst. 4 (2003), doi:10.1029/2002GC000339.
[42] W. Abouchami, A.W. Hofmann, S.J.G. Galer, F.A. Frey, J. Eisele, M. Feigenson, Lead isotopes reveal bilateral asymmetry and vertical continuity in the Hawaiian mantle plume, Nature 434 (2005) 851–856.
[43] E.H. Hauri, J.A. Whitehead, S.R. Hart, Fluid dynamics and geochemical aspects of entrainment in mantle plumes, J. Geophys. Res. 99 (1994) 24,275–24,300.
[44] K.H. Rubin, J.D. Macdougall, Th–Sr isotopic relationships in MORB, Earth Planet. Sci. Lett. 114 (1992) 149–157.
[45] M. Spiegelman, UserCalc: a web-based uranium series calculator for magma migration problems, Geochem. Geophys. Geosyst. 1 (2000), doi:10.1029/1999GC000030.
[46] V.J.M. Salters, J. Longhi, Trace element partitioning during the initial stages of melting beneath mid-ocean ridges, Earth Planet. Sci. Lett. 166 (1999) 15–30.